Smart Structures and Systems, *Vol. 28, No. 5 (2021) 699-709*
https://doi.org/10.12989/sss.2021.28.5.699

Jumps phenomenon elimination of a Duffing oscillator using pole placement control method

Reza Mahmoudi [1a], Hosein Ghaffarzadeh[*1] and T.Y. Yang [2b]

[1] *Faculty of Civil Engineering, University of Tabriz, Tabriz, Iran*
[2] *Department of Civil Engineering, University of British Columbia, Vancouver, Canada*

(*Received June 1, 2019, Revised March 17, 2021, Accepted September 30, 2021*)

Abstract. This paper presents a numerical and analytical study in the time-frequency domain to control the bifurcation and instability in a forced Duffing oscillator by a linear state feedback control. The proposed method evolves minimizing computational expenses of analytical approaches by an approximate method to suppress the responses of the dynamical system based on pole placement theory. The instability frequency range of Duffing oscillator is identified by approximate analytical methods. Bifurcation and jump points of Duffing oscillator are identified in the frequency domain by perturbation and harmonic balance methods for average and strong nonlinearity of the system, respectively. The Caughey method is used to linearize Duffing oscillator to solve system in the state space form. A linear state feedback controller with pole placement is applied to system in the time domain. The observed controlling force is added to approximate solution equation in frequency domain which vanished bifurcation length. The results reveal that the proposed method can be beneficial in reducing dynamic responses and eliminating jump points of system with high accuracy.

Keywords: bifurcation and jump; gain coefficient; harmonic balance; linearization; perturbation; pole placement

1. Introduction

Nonlinear ordinary differential equations are frequently used to model a broad range of complications in various scientific areas such as chemical, spring-mass systems, bending beams, resistor-capacitor-inductance circuits, pendulums, and the motion of a rotating mass around another body. Duffing oscillator, as a nonlinear system, which typically exhibits absorbing and unpredicted behavior such as bifurcation and chaos, is regularly used in the geometrical nonlinear fields. It is one of the most represented systems to model and identifies the behavior of nonlinear systems (Kovacic and Brennan 2011, Nayfeh *et al*. 1979).

This system, with an emphasis on cubic stiffness, is used to recognize mechanical and engineering system specifications and characteristics. Recently, the nonlinear process is one of the most significant challenges and is not easy to control. So nonlinear properties of system, dramatically change the solution due to some slight changes of valid parameters including time. Therefore, the issue becomes more difficult and hence, needs an ultimate solution. The main problem in the study of nonlinear systems is to find exact solutions and explicitly describe their behaviors. Thus, engineers and scientists require an efficient method to solution to these types of equations. To dispel the defects, many new analytical methods have been proposed nowadays. Approximate and analytical solutions such as Perturbation (Glendinning 1994), Harmonic Balance (Worden and Tomlinson 2001), averaging (Verhulst 1996), normal form transformation (Jezequel and Lamarque 1991) and Volterra series (Storer and Tomlinson 1993) are used to Study the nonlinearity in dynamic systems. The base of perturbation method (PM) as a classical method is a Taylor expansion which estimates the initial response of a system. And Harmonic Balance method (HBM) is a method for obtaining analytic approximations of its time-periodic solutions using truncated Fourier series.

There exist an essential difference between the phenomena, which oscillate in steady-state, and the phenomena governed by the linear differential equations. One of the principal concepts of nonlinear systems in the frequency domain is the bifurcation phenomenon which involves two critical points of jumping up and down in a Duffing system. This phenomenon occurs while solving the nonlinear system dynamics by higher-order frequency response function (FRF). Since the introduction of computer programming, researchers have used numerical and hybrid analytical-numerical approaches to study bifurcation in the Duffing systems. Peleg (1979) investigated a hardening isolation system with friction and viscous damping by introducing implicit equations to the jump-down and jump-up frequencies, and the amplitude of response at these frequencies. Murata *et al*. (1987) investigated a hardening system represented by the Duffing equation. They settled the jump frequencies numerically and presented their results graphically using the catastrophe theory. Friswell and Penny (1994) and Worden (1996)

*Corresponding author, Ph.D.,
E-mail: ghaffar@tabrizu.ac.ir
[a] M.Sc. Graduated, E-mail: r.mahmoudi.ac@gmail.com
[b] Ph.D., E-mail: yang@civil.ubc.ca

http://www.techno-press.org/?journal=sss&subpage=7
ISSN: 1738-1584 (Print), 1738-1991 (Online)

calculated the jump-up and jump-down frequencies of the Duffing oscillator with linear damping. In both studies, Harmonic Balance Method (HBM) was used to achieve the frequency response curves. Among the mentioned techniques, the analytical approach uses perturbation methods such as multiple scales which can be applied to weakly nonlinear systems (Brennan *et al*. 2008). Brennan *et al*. (2008) investigated the multiple scales and Harmonic balance method in the degree of nonlinearity and the response amplitude of systems. They showed the deficiency of two methods response in both states of weak and strong nonlinearity system.

The control of undesirable behaviors in nonlinear systems has also been addressed in recent studies. Following the work of Ott *et al*. (1990) on chaos control in 1990, an extensive variety of methods were introduced to study chaos and nonlinearity control in chaotic systems (Agiza and Yassen 2001, Chen and Lü 2002, Elabbasy *et al*. 2004, Lei *et al*. 2006, Mahmoud *et al*. 2007, Park 2005a, b, Uçar *et al*. 2006, Wang *et al*. 2003). Loria *et al*. (1998) have controlled a periodically applied Duffing equation with uncertainty in all parameters. They used a feedback PID-based controller and offered an adaptive tracking control to guarantee the global asymptotic convergence. Park (2006) introduced a novel synchronization of Genesio chaotic system via a back-stepping strategy. A great deal of research has been conducted on FRF domain control of systems in recent years. Ghandchi-Tehrani *et al*. (2015) reduced the FRF response system of a Duffing system by the pole placement method. They used a numerical harmonic balance method to get the length of the instability. Active controls have been widely studied and used as a rudimentary set to suppress Duffing oscillator chaotic response. Wu *et al*. (2015) stabilized a range of nonlinear strict-feedback systems with time-delay by an adaptive back-stepping neural controller. Efimov and Perruquetti (2016) used a discrete-time method to simulate the approximation solution of Duffing oscillator illustrate its nonlinear phases. Mahmoudi *et al*. (2019) controlled response of Duffing oscillator with linear structures, equipped with active tendons, by the sliding mode control (SMC) technique. Contreras-Lopez *et al*. (2019) reduced nonlinear response of civil structures by frequency characteristics. Baghaei *et al*. (2019) decreased response of the linear structure and eliminated chattering in the applied control force by using a combination of fuzzy logic control (FLC) and SMC methods.

During the last decade, passive control has been employed in designing an asymptotically stabilizing controller for chaotic nonlinear systems with real variables (Chen and Liu 2010).

For passive control of the Duffing oscillator, Beltran-Carbajal and Silva-Navarro (2014) implemented an active vibration absorption scheme to control the response.

In the present study, authors use the approximation analytical method by the perturbation and Harmonic Balance technique apply it to a hardening Duffing oscillator to obtain bifurcation and its length. Bifurcation length is defined as the distance of jump up and down points in the frequency domain. Linearization method is utilized to the feasibility of cubic stiffness solution in state space and consequently obtaining poles of Duffing system in the time domain. To get the gain matrix a closed-loop force feedback control is applied to the linearized Duffing mass-spring-damper system in the time domain. This obtained control force is added to PM and HBM to eliminate unstable branches in FRF. The proposed method presents the accuracy of approximate solution in comparison to the available numerical method in the frequency domain. The beginning point of instability in the bifurcation length is called the threshold of bifurcation, which can help to predetermine system instability in the high amplitude of excitation. The bifurcation threshold allows designers to set control intensity by requirements considering.

1.2 Proposed methodology

The purpose of the present paper is to achieve a safe situation of stability in a Duffing oscillator by the pole-placement control strategy. The schematic diagram of the proposed control process is shown in Fig. 1. First, bifurcation length is obtained by both PM and HBM methods. Then, Duffing system is linearized by the Caughy method. After that, the proposed control method is assigned to the resulting linear system to derive the gain coefficients. These coefficients are added iteratively in terms of a control law to nonlinear approximate solution equation (PM and HBM equations) of the system until the bifurcation is removed.

1.3 State of the art

Nature is nonlinear and the best way will be to deal with it with nonlinear approaches. Although, linear control has been successfully employed for decades. The problem with a linear system is that it may not be able to provide modern and advanced technology. Duffing oscillator is a nonlinear system that shows chaotic behavior in the bifurcation region. To address the bifurcation phenomenon, lengths of instability are obtained through applying PM and HBM methods to Duffing system. PM uses the Taylor expansion of Duffing equation to obtain the analytical approximate response in the weakly and averagely nonlinear systems. Also, HBM is an efficient method for strong nonlinearity systems with high excitation. The initial principle of HBM

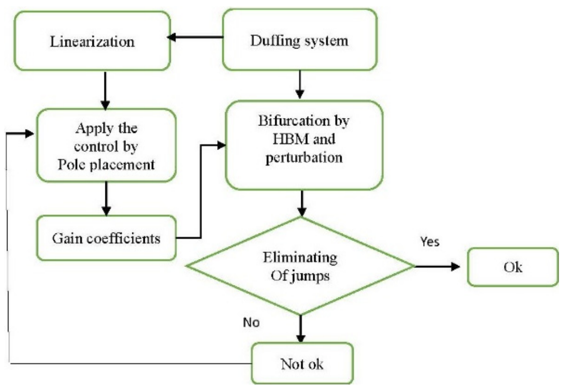

Fig. 1 The schematic diagram of the bifurcation control process

is to express the periodic solution in terms of the Fourier series with limited numbers of harmonics and substitute this expression to the dynamic equation. In this paper, PM and HBM are used to find jump points and the bifurcation length. To reduce the response of Duffing system, a pole placement control method by the closed-loop desired poles is utilized in the linearized equation. The gain matrix is obtained by pole placement application, then the gain coefficients are added to the initial equation. By solving the dynamic motion equation using PM and HBM, the amplitude of the FRF is reduced. Nonlinear FRF of dynamical system implies that the state trajectories with different initial conditions will converge to a unique bounded steady-state solution. A comparison of results with approximate analytical and numerical solutions indicate the excellent accuracy of the frequency response.

2. Analytical analysis of a Duffing oscillator

2.1 Perturbation method (PM)

Perturbation methods are classical methods that have been used for over a century to obtain approximate analytical solutions. The method has been successfully applied to differential equations. It is formulated by adding a “small” term to the mathematical description of the dynamical system. The approximate solution is obtained by expanding Taylor series in a small parameter (ε) and substituting them in the main equation. PM is a suitable approximate method to solve the weak and average nonlinear dynamical systems. Cubic stiffness of a Duffing oscillator denotes nonlinear term of the dynamic motion equation, which causes the chaotic behavior in the oscillator. The degree of nonlinearity determines type of approximate method to be applied Duffing system.

Fig. 2 illustrates the configuration of a Duffing oscillator as a nonlinear dynamical system. The motion equation of a Duffing oscillator subjected to an external excitation is written as

$$m\ddot{x} + c\dot{x} + kx + \gamma x^3 = F\cos(\Omega t) \tag{1}$$

where m, c, k and γ are the mass, damping coefficient, stiffness, and the nonlinear ratio of one degree-of-freedom Duffing system, respectively. F and Ω are the excitation amplitude and the frequency. System has hardening behavior for $\gamma > 0$ and softening behavior for $\gamma < 0$. In order to solve Eq. (1) by the perturbation method, a small parameter ($0 < \varepsilon < 1$) is introduced to consider the

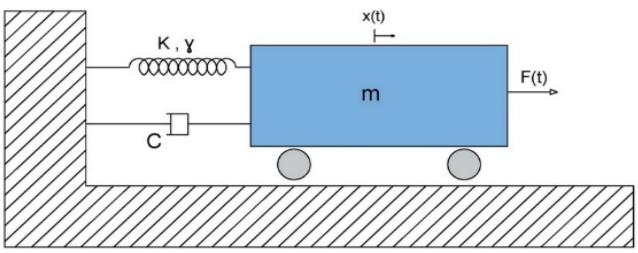

Fig. 2 Schematic diagram of the Duffing mechanical

nonlinear restoring and excitation forces in the perturbation form. The Epsilon ε is a variable amount which changes the amplitude and accuracy of the system. For an average nonlinear system, with $\varepsilon = 1$. For a dynamic system with a primary resonance (m = 1), Eq. (1) is written as

$$\ddot{x} + \omega_0 x = \varepsilon(F\cos\Omega t - 2\beta\omega_0 - \gamma x^3) \tag{2}$$

where β, ω_0 are the damping ratio and the natural frequency of system, respectively. Since ε is a small parameter, T_n as a time transition parameter, represent different time scales. In order to solve Eq. (2), x is expanded with respect to t and ε as

$$x(t,\varepsilon) = x_0(T_0,T_1) + x_1(T_0,T_0) + \cdots \tag{3}$$

where,

$T_0 = \varepsilon t_1$, $T_1 = \varepsilon t_1$, and Considering Ω as: $\Omega = \omega_0 + \varepsilon\sigma$. With σ as the perturbation frequency. Eq. (2) can be re-written with respect to the following derivatives $\frac{d}{dt} = \frac{\partial}{\partial T_0} + \frac{\partial}{\partial T_1} = D_0 + D_1$, as Eqs. (4) and (5)

$$D_0{}^2 x_0 + x_0 = 0 \tag{4}$$

$$\begin{gathered} D_1{}^2 x_1 + x_1 = -2D_0 D_1 x_0 - 2\beta D_0 x_1 - \gamma x_0{}^3 \\ +F\cos(T_0 + \sigma T_1) \end{gathered} \tag{5}$$

Solving Eqs. (4) and (5) gives

$$x_0(T_0,T_1) = A(T_1)e^{iT_0} + A^*(T_1)e^{-iT_0} \tag{6}$$

$$\begin{gathered} D_0 x_1 + x_1 = -i(2A' + 2\beta A)e^{iT_0} - 3\gamma A^2 A^* e^{iT_0} \\ -\gamma A^2 A^* e^{iT_0} - \gamma A^3 e^{3iT_0} \\ +\frac{F}{2}e^{iT_0}e^{i\sigma T_0} + c.c \end{gathered} \tag{7}$$

Where $A^*(T_1)$ is a complex conjugate, and $A(T_1)$ is a complex domain function obtained by equating the secular terms in Eq. (7) to zero

$$-i(2A' + 2\beta A) - 3\gamma A^2 A^* + \frac{F}{2}e^{i\sigma T_1} = 0 \tag{8}$$

Considering $A' = \frac{dA}{dT_1}$, Eq. (8) is solved as

$$A(T_1) = \frac{1}{2}a(T_1)e^{i\theta(T_1)} \tag{9}$$

where $a(T_1)$ and θ are the amplitude and the real values. By separating the real and complex parts of Eq. (9) and introducing the phase $\varphi = (\sigma T_1 - \theta)$, Eq. (9) is written as

$$\frac{da}{dT_1} = -\beta\omega_0 a + \frac{F}{2\omega_0}\sin\varphi \tag{10}$$

$$\frac{d\varphi}{dT_1} = \sigma - \frac{3\gamma}{8\omega_0}a^2 + \frac{F}{2\omega_0 a}\cos\varphi \tag{11}$$

Considering that the solutions of Eqs. (10)-(11) are fixed points with constant amplitude and phase, these equations can be re-written as

$$-\beta\omega_0 a+\frac{F}{2\omega_0}\sin\varphi=0 \tag{12}$$

$$\sigma-\frac{3\gamma}{8\omega_0}a^2+\frac{F}{2\omega_0 a}\cos\varphi=0 \tag{13}$$

The frequency response equation is obtained through squaring and adding Eqs. (12)-(13) in the form of

$$\left[(2\beta{\omega_0}^2)^2+(2\sigma\omega_0-\frac{3}{4}\gamma a^2)^2\right]a^2=F^2 \tag{14}$$

Where

$$\tan\varphi=\frac{-\beta\omega_0}{\sigma-\frac{3}{8}\gamma a^2} \tag{15}$$

Moreover, to obtain the stability point of the amplitude, Eq. (12) is rewritten as

$$\frac{\Omega}{\omega_0}=1+\left(\frac{3\gamma}{8{\omega_0}^2}\right)a^2\pm\sqrt{\frac{(\varepsilon F)^2}{(2{\omega_0}^2 a)^2}-(\varepsilon\beta)^2} \tag{16}$$

$$\lambda=-\beta\omega_0\pm\sqrt{-\left((\Omega-\omega_0)-\frac{3\gamma}{8\omega_0}a^2(\Omega-\omega_0)-\frac{9\gamma}{8}a^2\right)} \tag{17}$$

Based on Eq. (17), system stability is constrained to sign of the sum of squares for the lambda terms. For a positive value, the system is stable, otherwise, it is unstable.

To illustrate the solutions of Eqs. (16) and (17), an example of the jump phenomenon for weak nonlinearity by The Duffing oscillator system parameters and excitation amplitude as m = 1 kg, c = 0.1 N.s/m, k = 1 N/m, gamma = 0.1 N/m^3, F = 1 N is shown in Fig. 3. Amplitude of the steady-state displacement in the Fig. 3 for Duffing oscillator is solved in MATLAB.

Two states of Duffing oscillator, hardening and softening are seen in Fig. 3. Hardening and softening FRFs are bent to the right and left respectively. The stable and unstable branches of bifurcation are shown by solid and dashed-dot lines for each of the hardening and softening forms, respectively. Bifurcation phenomenon is dependant to the degree of nonlinearity. Therefore, in a system with high nonlinearity, it needs the strongest series for expansion of the term, because of chaos problems.

The analytical approximation response for hardening system in Fig. 3 showed in the right branch. The jumps phenomenon started from 1.41 to 4.7 rad/s for the jump up and the jump down points respectively. Fig. 4 shows the numerical response of bifurcation length for the hardening system. The dashed-dot line illustrates the bifurcation length which is started from 1.41 up to 4.7 rad/s in the frequency axis which validates the bifurcation length seen in Fig. 3.

2.2 Harmonic Balance method (HBM)

Analytical approximate PM can be applied to the weakly nonlinear systems, but to find jump points in the strongly nonlinear system its results are not accurate. Therefore, HBM technique is proposed as an approximate solution, in the form of $X=x_c\cos(\Omega t)+x_s\sin(\Omega t)$, where x_c, x_s are the steady-state response amplitudes according to Krack and Gross (2019). Considering the motion equation in Eq. (1) and $x_h=x_c\cos(\Omega t)+x_s\sin(\Omega t)$, the derivatives of the harmonic response are written as

$$\begin{aligned}\dot{x}_h&=-x_c\Omega\sin(\Omega t)+x_s\Omega\cos(\Omega t)\\ \ddot{x}_h&=-x_c\Omega^2\cos(\Omega t)+x_s\Omega^2\sin(\Omega t)\end{aligned} \tag{18}$$

By substituting Eq. (18) into Eq. (1) and considering the trigonometric identities required to expand the nonlinear term ${x_h}^3$ Eq. (18) yields

$$\begin{aligned}&((1-\Omega^2)x_c+\xi\Omega x_s+\frac{3}{4}\gamma({x_c}^3+x_c{x_s}^2)-F)\cos(\Omega t)\\ &+((1-\Omega^2)x_s+\xi\Omega x_c+\frac{3}{4}\gamma({x_s}^3+x_s{x_c}^2))\sin(\Omega t)\end{aligned} \tag{19}$$

By considering the terms with frequency Ω and neglecting the term with 3Ω in Eq. (18) according to Ansatz theory (Seemann and Gausmann 2001) and by setting Fourier coefficients to zero, Eq. (19) is formulated as

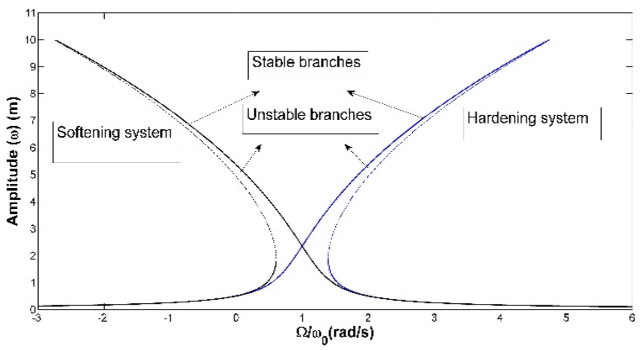

Fig. 3 Bifurcation branches for hardening and softening system

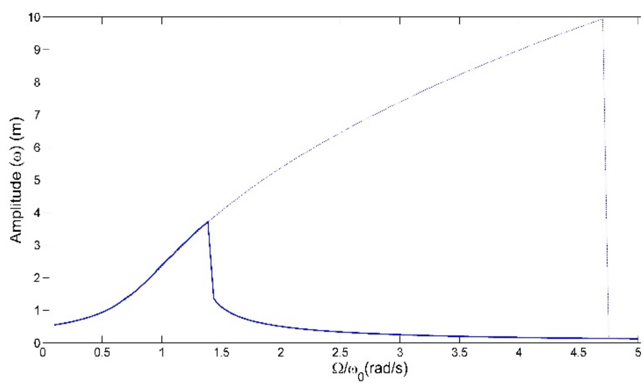

Fig. 4 Bifurcation length obtained from ODE45 solver

$$
\begin{aligned}
R_c(x_c,x_s) &= (1-\Omega^2)x_c + \xi\Omega x_c + \frac{3}{4}\gamma({x_c}^3 + x_c{x_s}^2) - F = 0 \\
R_s(x_c,x_s) &= (1-\Omega^2)x_s + \xi\Omega x_c + \frac{3}{4}\gamma({x_s}^3 + x_s{x_c}^2) = 0
\end{aligned} \tag{20}
$$

Where sum of R_c, R_s is the total steady-state response. This algebraic equation system governs the Fourier coefficients of the HBM approximation. By these assumptions, the HBM solution of the forced Duffing oscillator in frequency response is determined. For RFR analysis it can be mathematically stated as

$$R(x) = [R_c, R_c]^T = 0 \tag{21}$$

To obtain roots and the stability region of Duffing system, a polar coordinates transform is introduced as

$$
\begin{aligned}
&x_c = acos\theta, \quad x_s = asin\theta \\
&{x_c}^2 + {x_s}^2 = a^2
\end{aligned} \tag{22}
$$

where a is the response amplitude and θ is the phase lag between the response and the forcing parameter. Through substituting Eq. (22) into Eq. (20) and performing algebraic manipulations, the quadratic equation of Ω is obtained as

$$ {\Omega_{1,2}}^2 = 1 - \frac{\xi^2}{2} + \frac{3\gamma a^2}{4} \pm \sqrt{\left(\frac{F^2}{a^2} + \frac{\zeta^4}{4} - \zeta^2 - \frac{3\zeta^2\gamma a^2}{4}\right)} \tag{23}$$

Depending on the a (amplitude) parameter, Eq. (23) has zero, one, or two real-valued solutions for Ω^2. Resulting amplitude-frequency curves are derived as in Fig. 5 for example which mentioned in the perturbation method section. Considering Fig. 2 and comparing it with Fig. 5, it can be seen that the length of the bifurcation obtained from HBM method is less than PM technique. As mentioned, in the weak and average nonlinearity, PM is more accurate than HBM. However, in the strong nonlinearity, HBM is.

3. Linearization method

In this section, the Caughey method is utilized to linearize the motion equation of a Duffing system. The linearization is first to find the approximate poles of the linear form of Duffing oscillator. Then, the obtained poles are moved to stable location in the pole-zero diagram to control the system dynamics. A Pole-zero diagram is a graphical representation of a rational transfer function in the complex plane which helps to convey certain properties of the system. The linearization process must have an equilibrium point. The best choice for this point is one of three fixed points of the main Duffing oscillator in Eq. (1). The fixed point is the root of nonlinear differential equations. The fixed point or equilibrium point to linearization is chosen at the point (0, 0).

Considering the general form of Eq. (1) as

$$m\ddot{x} + f(x,\dot{x}) = F(t) \tag{24}$$

where $F(T)$ is a zero-mean Gaussian excitation and $f(x,\dot{x})$ is the nonlinear and linear parts of the system. A sensible strategy to linearize Eq. (24) is to minimize the average difference between the nonlinear and linear parts of the system as

$$J(x, c_{eq}, k_{eq}) = E[f(x,\dot{x}) - k_{eq}x] \tag{25}$$

where, k_{eq} is the equivalent linear stiffness; E and J stand for the mathematical expectation and evaluation criterion, respectively.

In order to minimize J, a derivative of Eq. (25) with respect to k_{eq} is written as

$$\frac{\partial J}{\partial k_{eq}} = 0 \tag{26}$$

Eq. (26) yields

$$
\begin{aligned}
&E[k_{eq}x^2 - xf(x,\dot{x}) + cx\dot{x}] \\
&= k_{eq}E[x^2] - E[xf(x,\dot{x}) + cE[x\dot{x}] = 0
\end{aligned} \tag{27}
$$

It comes of considering $E[x\dot{x}] = 0$ as a basic theorem in the stochastic processes, Eq. (27) becomes

$$k_{eq} = k + \frac{E[f(x,\dot{x},)]}{E[x^2]} \tag{28}$$

where, the expectation of the function $f(x,\dot{x})$ is considered as

$$E[f(x,\dot{x})] = \int_{-\infty}^{+\infty}\int_{-\infty}^{+\infty} \rho(x,\dot{x}) f(x,\dot{x})\, dx d\dot{x} \tag{29}$$

where $\rho(x,\dot{x})$ is the probability density function (PDF) of $x\, and\, \dot{x}$. However, the PDF is not known for general nonlinear systems. Thus, it is necessary to approximate $\rho(x,\dot{x})$ with $\rho_{eq}(x,\dot{x})$. Besides, regarding the basic theory of random vibration in linear systems (Dinca and Teodosiu 1973), PDF is written as

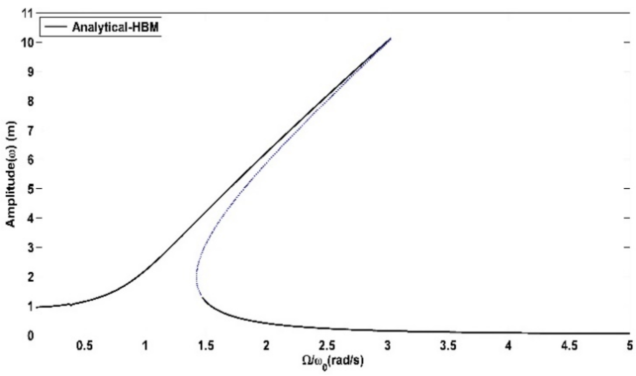

Fig. 5 Bifurcation of Duffing hardening system using HBM

$$p_{eq}(x_{eq}) = \frac{1}{\sqrt{2\pi v_{x_{eq}}}} exp\left(-\frac{{x_{eq}}^2}{2{v^2}_{x_{eq}}}\right) \quad (30)$$

$$p_{eq}(\dot{x}_{eq}) = \frac{1}{\sqrt{2\pi v_{\dot{x}_{eq}}}} exp\left(-\frac{{\dot{x}_{eq}}^2}{2v\dot{x}_{eq}}\right) \quad (31)$$

with the joint PDF written as

$$\begin{aligned} p_{eq}(x_{eq}, \dot{x}_{eq}) &= p_{eq}(x_{eq}) p_{eq}(\dot{x}_{eq}) \\ &= \frac{1}{\sqrt{2\pi} v_{x_{eq}} \sigma_{\dot{x}_{eq}}} exp\left(-\frac{{x_{eq}}^2}{2{v_{x_{eq}}}^2} - \frac{{\dot{x}_{eq}}^2}{2{v^2}_{x_{eq}}}\right) \end{aligned} \quad (32)$$

where V is the variance of the system excitation F, Thus, with $p_{eq}(x_{eq}, \dot{x}_{eq}) = p_{eq}(x_{eq}) p_{eq}(\dot{x}_{eq})$, Eq. (29) can be written

$$\begin{aligned} E[x\varphi(\dot{x})] &= \left(\int_{-\infty}^{+\infty} dx . p_{eq}(x) . x\right)\left(\int d\dot{x}\, p_{eq}(\dot{x}) \varphi(\dot{x})\right) \\ &= E[x] E[\varphi(\dot{x})] \end{aligned} \quad (33)$$

Since F(t) is considered as zero-mean Gaussian, it is concluded that

$$\mathrm{E}[x\varphi(\dot{x})] = 0 \quad \text{and} \quad \mathrm{E}[x] = 0 \quad (34)$$

Thus, Eq. (28) is obtained as

$$k_{eq} = k + \frac{1}{\sqrt{2\pi} {v^3}_{x_{eq}}} \int_{-\infty}^{+\infty} dx . x\phi(x)\, exp\left(-\frac{x^2}{2{v^2}_{x_{eq}}}\right) \quad (35)$$

The variances in the integrals of Eq. (35) are calculated based on the standard theory as (Newland 1993)

$$\begin{aligned} {v^2}_{x_{eq}} &= \int d\omega \left|H_{eq}(\omega)\right|^2 s_{xx}(\omega) \\ &= \int_{-\infty}^{+\infty} d\omega . \frac{s_{xx}(\omega)}{(k_{eq} - m\omega^2)^2 + c^2\omega^2} \end{aligned} \quad (36)$$

where $s_{xx}(\omega)$ is the standard deviation of F(t), which is assumed as a constant value P due to the zero-mean Gaussian type of the excitation.

Solving the integral of Eq. (36) yields

$${v^2}_{x_{eq}} = \bar{p} \int_{-\infty}^{+\infty} d\omega \frac{1}{(k_{eq} - m\omega^2) + c^2\omega^2} = \frac{\pi \bar{P}}{c k_{eq}} \quad (37)$$

Substituting Eq. (37) into Eq. (35) gives the equivalent stiffness as

$$k_{eq} = \frac{k}{2} + \frac{k}{2}\sqrt{1 + \frac{12\pi\gamma\bar{p}}{ck^2}} \quad (38)$$

In Eq. (38) c, k, γ are the, damping, linear and nonlinear stiffness and coefficients, respectively. $S_{xx} = \overline{p}$ in Eq. (36) which is a constant for a white zero mean Gaussian excitation (harmonic force) and assumed 0.02.

4. Pole placement control theory

Due to the gain coefficients requirement to a feedback control system, pole placement control method is considered.

Pole placement is a method employed in feedback control system theory to place the closed-loop poles of a plant in pre-determined locations in the poles-plane. Placing poles is desirable because the location of the poles corresponds directly to the eigenvalues of the system, which control the characteristics of the response of the system.

In this section, the application of the pole placement control method on a Duffing system is discussed. The motion equation of a linearized Duffing system subjected to a zero-mean Gaussian excitation can be written as

$$m\ddot{x}(t) + c\dot{x}(t) + k_{eq}x(t) = F(t) + u(t) \quad (39)$$

where, u(t) is the pole placement control law. The state space form of Eq. (39) can be expressed as

$$\dot{z}(t) = \boldsymbol{A}z(t) + F(t) + u(t) \quad (40)$$

where

$$z(t) = \begin{bmatrix} x \\ \dot{x} \end{bmatrix}_{2nx1}, \quad \boldsymbol{A} = \begin{bmatrix} \boldsymbol{O} & \boldsymbol{I} \\ -m^{-1}k_{eq} & -m^{-1}c \end{bmatrix}_{2nx2n} \quad (41)$$

A is a $2n \times 2n$ plant matrix of the system, and z is a $2n \times 1$ state vector. The eigenvalues of the system are given by the Eq. (42). If a state space formulation is adopted, these eigenvalues are obtained directly from the eigenvalues of matrix A, as indicated Eq. (43)

$$\lambda_i = -\omega_i\xi_i \pm j\omega_i\sqrt{1 - \xi_i^2} \quad (42)$$

$$det[\lambda\boldsymbol{I} - \boldsymbol{A}] = 0 \rightarrow \lambda_i \quad (43)$$

It is assumed that the control force u is determined by linear state feedback

$$u(t) = -\boldsymbol{G}_1 x(t) - \boldsymbol{G}_2 \dot{x}(t) = -\boldsymbol{G}z(t) \quad (44)$$

where G is the gain matrix calculated according to the desired eigenvalues (poles) of the controlled system. Replacing the force u into Eq. (40), the closed loop (controlled) system becomes

$$\dot{z}(t) = (\boldsymbol{A} - \boldsymbol{G})z(t) + f(t) \quad (45)$$

The new eigenvalues λ of the controlled system satisfy the following equation

$$det[\lambda I + G - A] = o \quad (46)$$

The state feedback design consists of selecting the gain matrix G so that the roots (eigenvalues) of Eq. (46) are at the desired locations. The desired eigenvalues λ of the controlled system also satisfy the equation

$$(\lambda - \lambda_{1c})(\lambda - \lambda_{2c})\dots(\lambda - \lambda_{nc}) = 0 \tag{47}$$

The controllable system can always be forced to have the desired eigenvalues by choosing the gain matrix G in such a way that Eq. (47) is identical to Eq. (46). A controllable system can always be forced to have the desired eigenvalues, however, this may not be practical, because the control gain G would be too large and a lot of energy would be required. In other words, because the range of values of the feedback gain would render the system oversensitive to noise or to modelling errors when the control law is implemented on the reconstructed state from an observer's point of view. These robustness aspects are extremely important and dominate the controller design, so the successful application of the pole placement algorithm requires correct selection of the controlled system eigenvalues from the part of the designing system.

The eigenfrequencies of the uncontrolled system are moved to the left region of the main complex phase after the selection of the eigenfrequencies of controlled system. And keeping the damping ratios the same, its eigenvalues or the poles of the controlled system are given by Eq. (48).

$$\lambda_{ci} = -\omega_i \xi_{ci} \pm j\omega_{ci}\sqrt{1 - \xi_{ci}^2} \tag{48}$$

Here to reduce the response of Duffing system in state-space first, the poles of open-loop system are found, then the desired poles are applied to the linearized system.

5. Numerical example

5.1 Example 1- averagely nonlinear system control by PM solution

In this section a hardening Duffing oscillator is considered to illustrate the Jump phenomenon and its removal by proposing the pole placement control method. For system parameters as m = 1, c = 0.1, k = 1, gamma = 0.1, F = 1, Eq. (2) is expressed as

$$\ddot{x} + 0.1\dot{x} + 1x + 0.1x^3 = 1\cos(\Omega t) \tag{49}$$

Using the perturbation method, bifurcation is illustrated in Fig. 6 with respect to Eq. (16). Fig. 6 shows the jump phenomenon and the bifurcation length which its range started from jump-down (square marked) to jump-up (circle marked) points with the length of $\Delta\omega = 4.7 - 1.41 = 3.29\,rad/s$. The dash-dot and solid lines indicate the unstable and stable branches, respectively, meaning that the bifurcation is located in an unstable range.

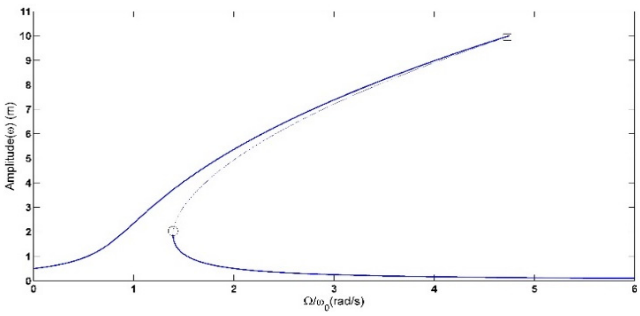

Fig. 6 Jumps phenomenon of Duffing oscillator

The time histories of dynamic responses associated with Eq. (49) are also depicted in Fig. 7.

To remove the Jump phenomenon and decrease amplitude response by pole placement control method, the proposed linearization method with p = 0.02 in Eq. (44) is utilized to derive the linearized motion equation as

$$k_{eq} = \frac{1}{2} + \frac{1}{2}\sqrt{1 + \frac{12 * \pi * 0.1 * 0.02}{0.1 * 1^2}} \tag{50}$$

where $k_{eq} = 1.17N/m$. The error of original and the linearized system response is less than 3% which is accepted.

The state space form of Eq. (49) is written as

$$\boldsymbol{A} = \begin{bmatrix} \boldsymbol{0} & 1 \\ -1.17 & -0.1 \end{bmatrix}_{2x2} \tag{51}$$

where the open-loop poles of system are

$$\lambda = -0.05 \pm j1.08 \tag{52}$$

Using pole placement control method, the desired poles are derived as

$$\lambda = -0.25 \pm j1.32 \tag{53}$$

The gain coefficients are obtained as in Eq. (54) to add PM and HBM equations.

$$G = [0.5825 \quad 0.3918] \tag{54}$$

Controlled dynamic responses of the Duffing system are depicted and compared with the uncontrolled correspondences in Fig. 9. The displacement responses are also shown in Fig. 9 indicating that the responses are reduced by 60%. Comparing responses in Figs. 7 and 9 clearly illustrates the efficiency of the proposed control method in reducing dynamic response.

Fig. 8 shows a pole-zero diagram with the location of poles for uncontrolled and controlled systems. In this figure,

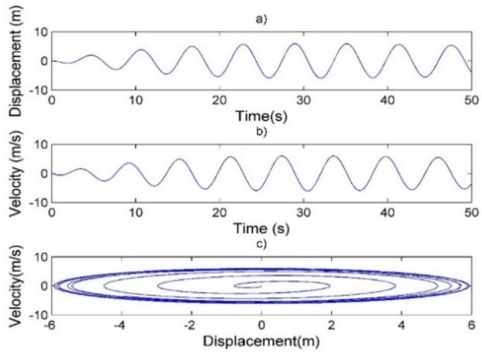

Fig. 7 Response of uncontrolled system: (a) displacement; (b) velocity; (c) phase portrait

uncontrolled and controlled system are marked with “square” and “circular” shapes respectively. Hence any moving of the poles toward the right-hand side will bring the system closer to the unstable region. Similarly, poles moving toward the left-hand side can be said to make the system “more stable.” It is evident that by applying the pole placement control method, poles are moved to a stable position.

The control force-time history is also shown in Fig. 11 where the amplitude of the control force is significant in comparison with the response reduction due to dynamic system.

Finally, in order to remove the Jump points in the bifurcation region of Fig. 6, the proposed control is added to Eq. (50) as follows

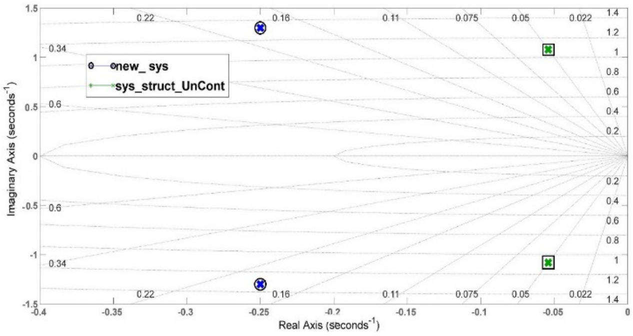

Fig. 8 Open and closed loop poles - (□) square points (open loop) and (O) circular poles (closed loop)

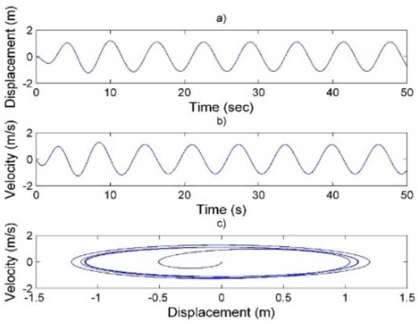

Fig. 9 Response of the controlled system - a) displacement; b) velocity; c) phase portrait

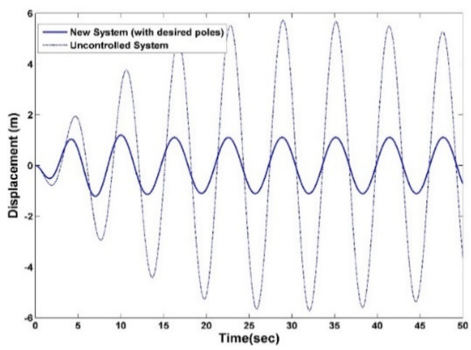

Fig. 10 Time history of controlled and uncontrolled displacements

$$
\begin{aligned}
&\ddot{x} + 0.1\dot{x} + x + 0.1x^3 \\
&= 1\,cos(\Omega t) + (-0.5825x - 0.3918\dot{x})
\end{aligned} \tag{55}
$$

Fig. 13 illustrates the frequency response of Duffing oscillator after Solving Eq. (55) via PM. The unstable branches are removed and compared to Fig. 5 as an uncontrolled approximate solution, the Jump phenomenon is vanished.

However, despite Jump removal, the instability in bifurcation threshold still remains as an important point which is needed to be addressed. Fig. 14 shows the decreased frequency response of a system, but while there is small instability with dash-dot points. This small part of instability shows the threshold of bifurcation. In order to vanish the instability, pole placement control strategy is formulated by the new poles. The jump threshold poles and related gain coefficients are obtained $\lambda = -0.15 \pm j1.2$ and $G = 0.2925 \;\; 0.1918$ respectively.

As shown in Fig. 14, a small part of the bifurcation

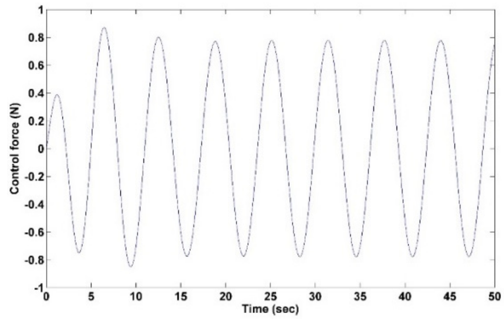

Fig. 11 Time history of control force

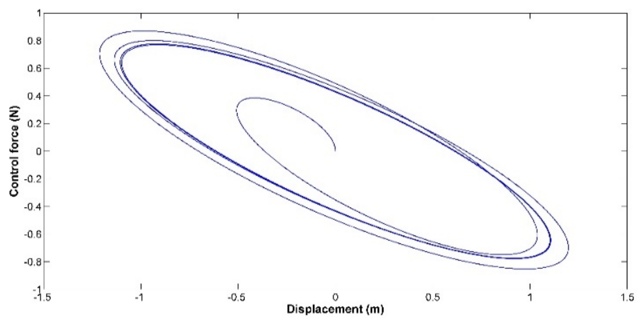

Fig. 12 Control force-displacement phase

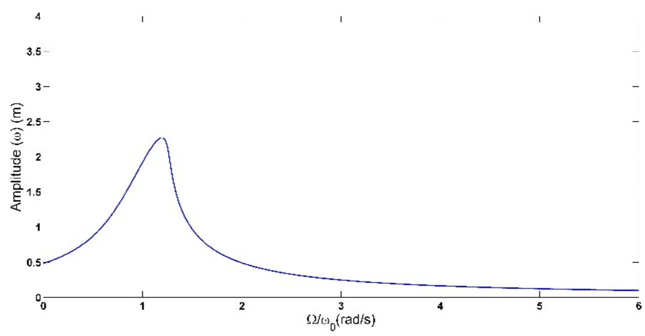

Fig. 13 Stable frequency response for Duffing oscillator

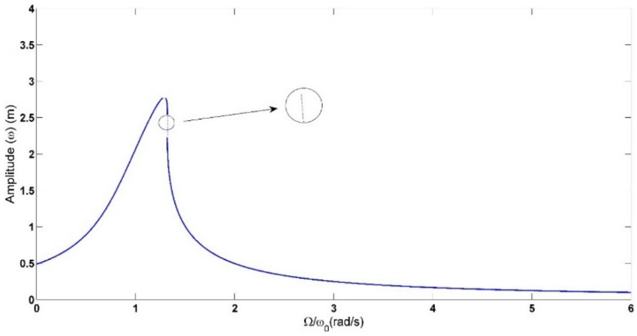

Fig. 14 Bifurcation threshold of Duffing oscillator

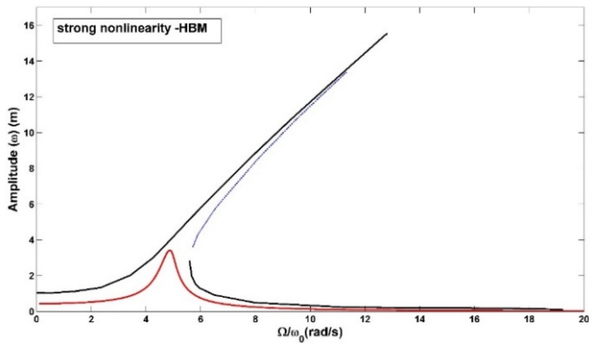

Fig. 15 Bifurcation phase and controlled response using HBM

length is not eliminated. By adding more control force or increasing the gain coefficients amount, that part will have vanished.

5.2 Example 2 – Strong nonlinearity system control by HBM solution

As mentioned, HBM response accuracy is more than PM technique in a strong nonlinearity system. By considering the system parameters m = 1, c = 0.1, k = 20, gamma = 0.8, and F = 20 for strong nonlinearity according to Ghandchi-Tehrani *et al*. (2015) and substituting in Eq. (19), the amplitude response of Duffing system and bifurcation length is obtained. As shown in Fig. 15, the black line branches are a stable form of a strongly nonlinear system. Control force is applied to the system for stabilizing of Duffing system which is seen by the red line in Fig. 15. The open-loop poles and desired poles of the system are $\lambda = -0.05 \pm 12.85j$ $\lambda = -0.35 \pm 9j$ respectively. Then the gain matrix (G) of system is obtained G = [60.97 0.2511]. The amplitude reduction of strong nonlinearity system ensures the performance of structure against high excitations. Fig. 16 shows the time domain uncontrolled and controlled system using pole placement algorithm. As it can be seen, initial response is reduced by more than 60%. The strong nonlinear system response is shifted to the forward by increasing the stiffness coefficient that is related to the gain matrix. However, HBM as an efficient method to find the accurate response, has a strong role in nonlinear mechanical systems.

Furthermore, the effectiveness and practicality of

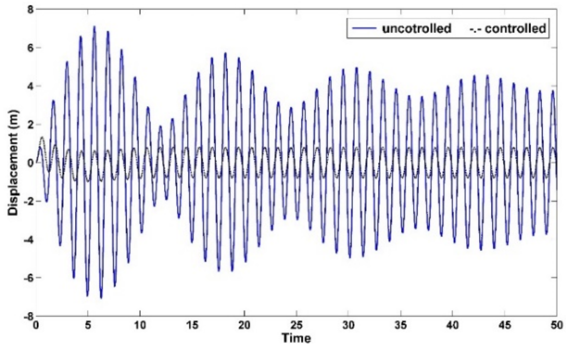

Fig. 16 uncontrolled and controlled response using pole placement

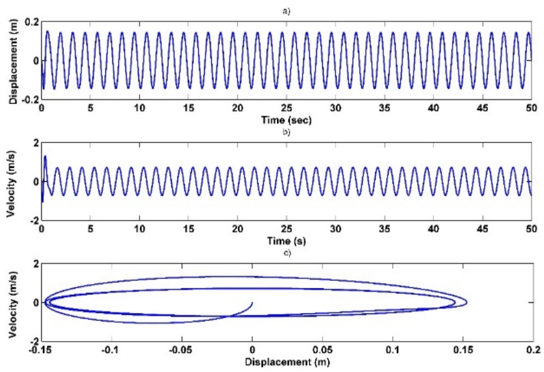

Fig. 17 Response of the controlled system using sliding mode - a) displacement; b) velocity; c) phase portrait

Duffing system response reductions in dynamic vibrations are evaluated by another control method as Sliding mode control (SMC). SMC is more powerful to reduce the response of Duffing system in the time domain. Considering sliding coefficients $S = [8.49\ \ 1]$ and $u(x,t) = -(SB)^{-1}SAz - \zeta sgn(\sigma(z))$ as a control force, the linearized system response is decreased (Mahmoudi *et al*. 2019). $\sigma(z) = 8.49x + \dot{x}$ is the sliding surface and, η is imparts discontinuity to control force action across the sliding surface. The equivalent stiffness obtained $K_{eq} = 20.15$. Fig. 17 shows the responses of Duffing system using sliding mode control. SMC enhanced the response of system by comparing pole placement control method. Since the SMC is a nonlinear control method and variable structure and it hasn't gain coefficients for controlled system, it can't be applied to an approximate analytical equation directly.

6. Conclusions

In this paper, an analytical approach, which is based on FRFs, is presented to determine the feedback control gains required for controlling bifurcation and instability in the oscillation of Duffing type nonlinear systems. The perturbation multi-scale approximation and harmonic balance methods were used as analytical tools to obtain instability and bifurcation points of the Duffing system.

First PM was used to the average nonlinear system and, HBM was applied to the strong nonlinearity Duffing oscillation. The difference between both systems was shown in the bifurcation results. The efficiency of HBM was noticeable under the high excitation that occurs in the civil structures.

In the next stage, linearization was applied to convert Duffing equation into an equal linear system. The linearized Duffing system was used as an exemplary system to implement the pole placement control algorithm to control the bifurcation, stability and reduce the response. Results of applying the proposed strategy show that system response decreased by more than 60 percent in the controlled system. At the final stage, the appropriate gain coefficient was obtained and then applied to the Duffing oscillator to find the controlled bifurcation position and demonstrate that jump points have been eliminated in the controlled system.

The purpose of the pole placement algorithm is to observe the elimination of the jump points. Nevertheless, the SMC as a nonlinear control algorithm reduced the uncontrolled response more than 80 percent.

In addition, feasibility of the proposed method is finding the bifurcation threshold. The bifurcation threshold is a confidential amount in process of a nonlinear Duffing oscillator controlling. The salient advantage of this method lies its ability to obtain reasonable results by consideration of the designing requirements for dynamical systems with less computational expenses.

References

Agiza, H.N. and Yassen, M.T. (2001), "Synchronization of Rossler and Chen chaotic dynamical systems using active control", **278**(4), 191-197. https://doi.org/10.1016/S0375-9601(00)00777-5

Baghaei, K., Ghaffarzadeh, H., Hadigheh, A. and Dias-da-Costa, D. (2019), "Chattering-free sliding mode control with a fuzzy model for structural applications", *Struct. Eng. Mech., Int. J.*, **69**(3), 307-315. http://doi.org/10.12989/sem.2019.69.3.307

Beltran-Carbajal, F. and Silva-Navarro, G. (2014), "Active vibration control in Duffing mechanical systems using dynamic vibration absorbers", *J. Sound Vib.*, **333**, 3019-3030. https://doi.org/10.1016/j.jsv.2014.03.002

Brennan, M.J., Kovacic, I., Carrella, A. and Waters, T.P. (2008), "On the jump-up and jump-down frequencies of the Duffing oscillator", *J. Sound Vib.*, **318**, 1250-1261. https://doi.org/10.1016/j.jsv.2008.04.032

Chang, R.J. (2017), "Extension of nonlinear stochastic solution to include sinusoidal excitation illustrated by Duffing oscillator", *J. Computat. Nonlinear Dyn.*, **12**(5), 051030. https://doi.org/10.1115/1.4037105

Chen, X. and Liu, C. (2010), "Passive control on a unified chaotic system", *Nonlinear Anal.: Real World Applicat.*, **11**, 683-687. https://doi.org/10.1016/j.nonrwa.2009.01.014

Chen, S. and Lü, J. (2002), "Synchronization of an uncertain chaotic system via adaptive control", *Chaos Solit. Fract.*, **14**, 643-647. https://doi.org/10.1016/S0960-0779(02)00006-1

Contreras-Lopez, J., Ornelas-Tellez, F. and Espinosa-Juarez, E. (2019), "Nonlinear optimal control for reducing vibrations in civil structures using smart devices", *Smart Struct. Syst, Int. J.*, **23**(3), 307-318. http://doi.org/10.12989/sss.2019.23.3.307

Dinca, F. and Teodosiu, C. (1973), "Nonlinear and Random Vibrations", *SIAM Review*, **17**(3), 578.

Efimov, D. and Perruquetti, W. (2016), "On condition of oscillations and multi-homogeneity", *Math. Control Signals Syst.*, **28**(1), 1-37. https://doi.org/10.1007/s00498-015-0157-y

Elabbasy, E.M., Agiza, H.N. and El-Dessoky, M.M. (2004), "Synchronization of modified Chen system", *Int. J. Bifurc. Chaos*, **14**, 3969-3979. https://doi10.1142/S0218127404011740

Friswell, M.I. and Penny, J.E.T. (1994), "The accuracy of jump frequencies in series solutions of the response of a Duffing oscillator", *J. Sound Vib.*, **169**(2), 261-269. https://doi 10.1006/jsvi.1994.1018

Ghandchi-Tehrani, M., Wilmshurst, L.I. and Elliott, S.J. (2015), "Bifurcation control of a Duffing oscillator using pole placement", *J. Vib. Control*, **21**(14), 2838-2851. https://doi.org/10.1177/1077546313517586

Glendinning, P. (1994), *Stability, Instability and Chaos: an Introduction to the Theory of Nonlinear Differential Equations*, Cambridge University Press, Cambridge, UK.

Jezequel, L. and Lamarque, C.H. (1991), "Analysis of nonlinear dynamic systems by the normal form theory", *J. Sound Vib.*, **149**(3), 429-459. https://doi.org/10.1016/0022-460X(91)90446-Q

Kovacic, I. and Brennan, M.J. (2011), *The Duffing equation: nonlinear oscillators and their behaviour*, John Wiley, London, UK.

Krack, M. and Gross, J. (2019), *Harmonic balance for nonlinear vibration problems*, Springer International Publishing. https://doi.org/10.1007/978-3-030-14023-6

Lei, Y., Xu, W., Shen, J. and Fang, T. (2006), "Global synchronization of two parametrically excited Systems using active control", *Chaos Solit. Fract.*, **28**, 428-436. https://doi.org/10.1016/j.chaos.2005.05.043

Loria, A., Panteley, E. and Nijmeijer, H. (1998), "Control of the chaotic Duffing equation with uncertainty in all parameters", *IEEE Transact. Circuits Syst. I: Fundamental Theory and Applications*, **45**(12), 1252-1255. http://doi.org/10.1109/81.736558

Luo, X.S., Zhang, B. and Qin, Y.H. (2010), "Controlling chaos in space-clamped FitzHugh–Nagumo neuron by adaptive passive method", *Nonlinear Anal.: Real World Applicat.*, **11**, 1752-1759. https://doi.org/10.1016/j.nonrwa.2009.03.029

Mahmoud, G.M., Aly, S.A. and Farghaly, A.A. (2007), "On chaos synchronization of a complex two coupled dynamos system", *Chaos Solit. Fract.*, **33**, 178-187. https://doi.org/10.1016/j.chaos.2006.01.036

Mahmoudi, R., Ghaffarzadeh, H., Ahani, E. and Katebi, J. (2019), "Sliding mode control of linear structures and a Duffing system using active tendons", *Proceedings of the Institution of Civil Engineers – Eng. Computat. Mech.*, **172**(3), 106-117. https://doi.org/10.1680/jencm.18.00033

Murata, A., Kume, Y. and Hashimoto, F. (1987), "Application of catastrophe theory to the forced vibration of a diaphragm air spring", *J. Sound Vib.*, **112**(1), 31-44. https://10.1016/S0022-460X(87)80091-3

Nayfeh, A.H., Mook, D.T. and Holmes, P. (1980), *Nonlinear Oscillations*, Wiley, New York, USA.

Newland, D.E. (1993), *Introduction to Random Vibrations*, Spectral and Wavelet Analysis, New York: Longman.

Ott, E., Grebogi, C. and Yorke, J.A. (1990), "Controlling chaos", *Phys. Rev. Lett.*, **64**(11), 1196-1199. https://doi.org/10.1103/PhysRevLett.64.1196

Park, J.H. (2005a), "Chaos synchronization of a chaotic system via nonlinear control", *Chaos Solit. Fract.*, **25**, 579-584. https://doi.org/10.1016/j.chaos.2004.11.038

Park, J.H. (2005b), "On synchronization of unified chaotic systems via nonlinear control", *Chaos Solit. Fract.*, **25**, 699-704. https://doi.org/10.1016/j.chaos.2004.11.031

Park, J.H. (2006), "Synchronization of Genesio chaotic system via back-stepping approach", *Chaos Solit. Fract.*, **27**, 1369-1375. https://doi.org/10.1016/j.chaos.2005.05.001

Peleg, K. (1979), "Frequency response of non-linear single degree-of-freedom systems", *Int. J. Mech. Sci.*, **21**, 75-84. https://doi.org/10.1016/S0022-460X(85)80150-4

Seemann, W. and Gausmann, R. (2001), "A note on the strong nonlinear behavior of piezoceramics excited with a weak electric field", *SPIE Smart Struct. Mater.*, **4333**, 131-140. https://doi.org/10.1117/12.432749

Storer, D.M. and Tomlinson, G.R. (1993), "Recent developments in the measurement and interpretation of higherorder transfer functions from nonlinear structures", *Mech. Syst. Signal Process.*, **7**(2), 173-189. https://doi.org/10.1006/mssp.1993.1006

Uçar, A., Lonngren, K.E. and Bai, E.W. (2006), "Synchronization of the unified chaotic systems via active control", *Chaos Solit. Fract.*, **27**, 1292-1297. https://doi.org/10.1016/j.chaos.2005.04.104

Verhulst, F. (1996), *Nonlinear Differential Equations and Dynamical Systems*, Springer, New York, USA.

Wagg, D. and Neild, S. (2010), *Nonlinear Vibration with Control*, Springer, New York, USA.

Wang, Y., Guan, Z.H. and Wang, H.O. (2003), "Feedback and adaptive control for the synchronization of Chen system via a single variable", *Phys. Lett. A*, **312**, 34-40. https://doi.org/10.1016/S0375-9601(03)00573-5

Worden, K. (1996), "On jump frequencies in the response of a Duffing oscillator", *J. Sound Vib.*, **198**(4), 522-525. https://doi.org/10.1006/jsvi.1996.0586

Worden, K. and Tomlinson, G.R. (2001), *Nonlinearity in Structural Dynamics, Detection, Identification and Modelling*, University of Sheffield, UK.

Wu, J., Chen, W., Yang, F., Li, J. and Zhu, Q. (2015), "Global adaptive neural control for strict-feedback time- delay systems with predefined output accuracy", *Inform. Sci.*, **301**, 27-43. https://doi.org/10.1016/j.ins.2014.12.039

HJ